Research on Commutating Over-Voltage Protection for ITER Poloidal Field Converter

Fengwei Zha, Zhiquan Song, Fu Peng, Ling Dong, and Min Wang

***Abstract*— This paper presents the commutating over-voltage snubber circuit design method of a thyristor converter that is applied to the International Thermonuclear Experimental Reactor poloidal field-converter module. In the course of poloidal field ac/dc converter normal operation, large transient surges called commutating over-voltages may be generated internally during the commutating process of thyristor, which poses a severe threat to system reliability and needs to be suppressed. In this paper, based on the analysis of reverse recovery transient of the parallel thyristors, the turn-off model of the PF converter thyristor is created and analytical expressions are derived, including the over-voltage crest value and the maximum over-voltage rise rate. Utilizing the analysis results, a systematic approach to the RC snubber circuit design is described.**

***Index Terms*— Ac/dc converter, commutating over-voltage, International Thermonuclear Experimental Reactor (ITER), poloidal field (PF), RC snubber circuit.**

I. Introduction

THE International Thermonuclear Experimental Reactor (ITER) is an international nuclear fusion research and engineering project that aims to demonstrate that it is possible to produce commercial energy from fusion.

The poloidal field (PF) converter module is an important part of ITER equipment, which should realize the function of the plasma shape and position control in vertical and horizontal directions [1]–[3].

In the course of PF converter-module normal operation, large transient surges called commutating over-voltages may be generated internally during the commutating process of thyristor, which poses a severe threat to the system reliability and needs to be suppressed. In this paper, based on the analysis of reverse recovery transient of the parallel thyristors, the turn-off model of the PF converter thyristor is created, and a systematic method to the RC snubber circuit design is described.

Manuscript received December 10, 2012; accepted March 20, 2013. Date of publication April 25, 2013; date of current version May 6, 2013. This work was supported by the International Thermonuclear Experimental Reactor Project of China under Grant 2008 GB104000.

F. Zha, Z. Song, and F. Peng are with the Institute of Plasma Physics, Chinese Academy of Science, Hefei 230031, China (e-mail: fengweizha@ipp.ac.cn; zhquansong@ipp.ac.cn; fupeng@ipp.ac.cn).

L. Dong and M. Wang are with the China International Nuclear Fusion Energy Program Execution Center, Beijing 100862, China (e-mail: lindongfr@gmail.com; wangm@iter.china).

Color versions of one or more of the figures in this paper are available online at http://ieeexplore.ieee.org.

Digital Object Identifier 10.1109/TPS.2013.2255896

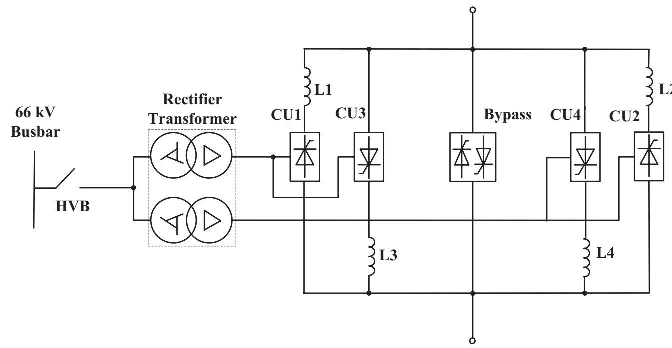

Fig. 1. Topology of PF converter module.

II. Converter Module and Snubber Design Requirements

The basic scheme of PF converter module is shown in Fig. 1 [4]. It is designed at 55-kA current and contains two transformers with 30-degree phase shift between secondary winding voltages to provide 12-pulse converter operation. The converter unit CU1, CU2 and anti-parallel unit CU3, CU4 are decoupled by dc inductors, performing four-quadrant operation. The PF converter module parameters are listed in Table I.

Thyristors are very sensitive to over-voltage just as other semi-conductor devices. High commutating over-voltage may cause permanent damage to the thyristor. Moreover, if voltage-rise rate (dv/dt) of thyristor in bridges CU1 and CU2 is high enough, it can turn on the thyristor in anti-parallel bridges CU3 and CU4, even though a turn-on is not intended. Therefore, the RC snubber circuit is required to keep the commutating over-voltage and dv/dt below a maximum allowable value, which is specified by the thyristor manufacturer. In addition, the reduction of the snubber power loss should be taken into consideration.

III. Thyristor Turn-Off Model

A. Single Thyristor Turn-Off Model

The transient of reverse recovery is one of the important research objects about thyristor electrical characteristics. Several reverse recovery models have been proposed previously. The macro model [5], [6] is considered overly complex and difficult to implement. The lumped-charge model [7] and the hyperbolic secant function model [8] are not easily implemented in simulation packages and required knowledge of parameters is not available to device users. The switch models [9], [10] are easy to use but not to address the

TABLE I
PF CONVERTER MODULE PARAMETERS

Parameter	Value
Transformer rated power	39 MVA
Transformer primary-rated voltage	66 kV
Transformer secondary-rated voltage	1 kV
Transformer leakage inductance	13 μH
Circuit stray inductance	2 μH
Thyristor type	ABB52U5200
Thyristor parallel number	12
Dc reactor inductance	200 μH

reverse recovery adequately. The exponential function model has been most commonly used over the past 20 years because its accuracy meets the engineering requirements, and the model parameter is easy to obtain from the reverse recovery characteristic curve provided by the manufacturer [10]–[14].

Fig. 2 shows typical current waveforms of single thyristor during reverse recovery time. I_F is the peak forward current, which begins to decrease and cross zero at $t = 0$, depending on the change of external circuit. After $t = 0$, the thyristor current continues to decreases at the same rate K because the excess-carriers cannot decay immediately. At $t = T_1$, the reverse current reaches its maximum value I_{rm}; after $t = T_1$, the thyristor recovers the reverse-blocking capability, and the current falls to zero. Because of the series inductance of the thyristor circuit, large transient surge V_c is produced, which is called commutating over-voltage.

The reverse recovery current i_r can be approximated by a waveform with constant slope K from zero to peak reverse current, followed by an exponential decay curve with time constant τ [12]–[14]. The peak reverse current I_{rm} and reverse charge Q_{rr}, which define the reverse recovery behavior, can be obtained from the device data sheet. Therefore, the reverse recovery current i_r can be modeled as [14]

$$\begin{cases} i_r = I_{\text{rm}} e^{-\frac{t-T_1}{\tau}} \\ \tau = \frac{Q_{\text{rr}}}{I_{\text{rm}}} - \frac{I_{\text{rm}}}{2\text{K}}. \end{cases} \tag{1}$$

B. Parallel Thyristors Turn-Off Model

In the nuclear fusion field, the thyristors often need to be connected in parallel to undertake large current, so it is necessary to study the reverse recovery transient under the condition of thyristors connected in parallel.

Suppose two thyristors V_1 and V_2 work independently, there will be two peak values of the reverse recovery current $I_{\text{rm}1}$, $I_{\text{rm}2}$, and two reverse recovery charges $Q_{\text{rr}1}$ and $Q_{\text{rr}2}$ correspond with decreased rates of each thyristor respectively.

Fig. 3 shows schematic drawing of reverse recovery current waveform of parallel thyristors. When the two thyristors work in parallel, the moment that reverses recovery current reaches its maximum value depends on the the decrease rate of the thyristor current.

However, the parallel thyristors circuit parameters cannot be completely symmetrical, so each thyristor current cannot enter the reverse recovery process at the same time. Assume that the reverse current of the thyristor V_1 reaches its peak value firstly and then, the thyristor V_1 recovers the reverse blocking

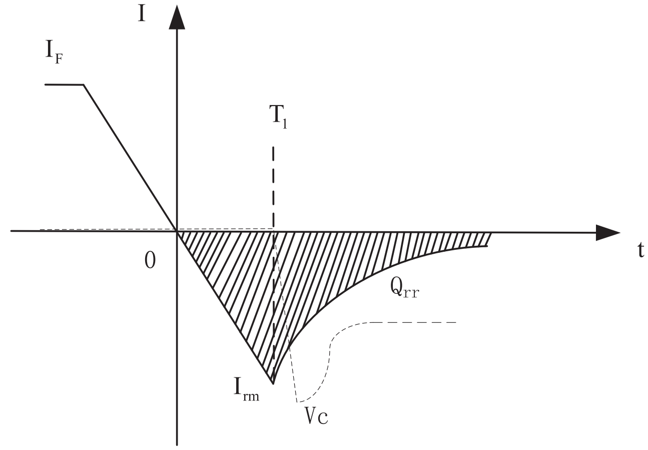

Fig. 2. Reverse recovery current waveform of single thyristor.

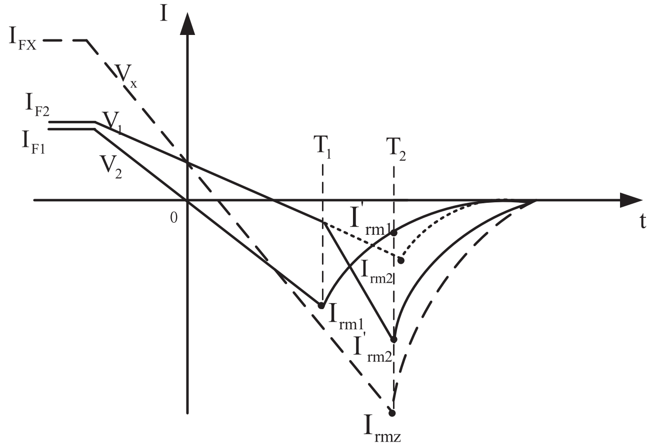

Fig. 3. Reverse recovery current waveform of parallel thyristors.

capability; the reverse current of the thyristor V_2 does not reaches its peak value yet, the thyristor V_2 keep on conducting, and the current of the thyristor V_1 is transferred to thyristor V_2, which accelerates the thyristor V_2 reverse-recovery current decrease rate. In fact, there is no commutating over-voltage across thyristor V_1 during the time of T_1–T_2 because the total reverse recovery current does not decrease yet. At the moment of T_2, when the thyristor V_2 reaches the peak value $I_{\text{rm}2}$ instead of $I_{\text{rm}2}$, and the thyristor V_1 reverse recovery current decreases to the value $I'_{\text{rm}1}$, then, the total reverse recovery current decays and the commutating over-voltage is produced.

It is unnecessary is to calculate how much reverse recovery current shifts from thyristor V_1 to V_2 because the commutating over-voltage value is affected by the total reverse recovery current of V_1 and V_2. Obviously, the total reverse recovery current is unaffected by the internal current-transfer process between two thyristors, the same as to the total reverse recovery charge. Equation (2) can be deduced as follows:

$$\begin{cases} I'_{\text{rm}1} + I'_{\text{rm}2} = I_{\text{rm}1} + I_{\text{rm}2} \\ Q'_{\text{rr}1} + Q'_{\text{rr}2} = Q_{\text{rr}1} + Q_{\text{rr}2}. \end{cases} \tag{2}$$

If two thyristors V_1 and V_2 are assumed as one thyristor V_x, it is easy to know that the reverse recovery current peak value of V_x is $I_{\text{rm}1} + I_{\text{rm}2}$, and the reverse recovery charge of V_x is $Q_{\text{rr}1} + Q_{\text{rr}2}$; so, the reverse recovery current of thyristor V_x

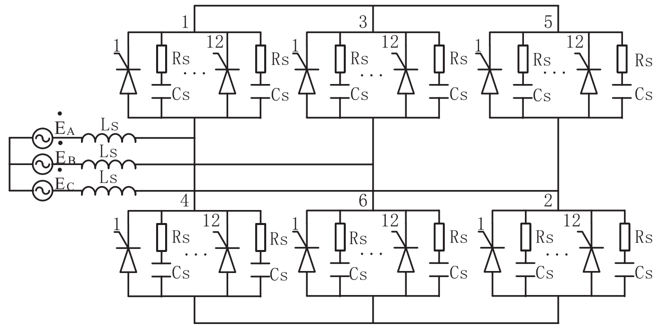

Fig. 4. Topology of converter unit.

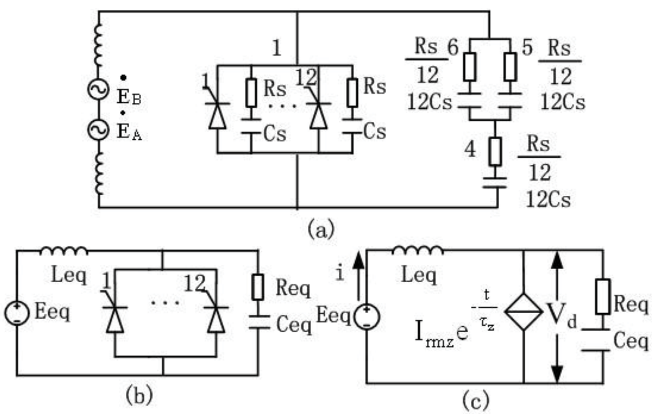

Fig. 5. Commutating equivalent circuits.

can be modeled by using (1). Simultaneously, as for n parallel thyristors, the total reverse recovery current can be modeled as

$$\begin{cases} i_{\mathrm{rmz}} = I_{\mathrm{rmz}} e^{-\frac{t}{\tau_z}} \\ K_z = K_1 + K_2 + \cdots K_n \\ I_{\mathrm{rmz}} = I_{\mathrm{rm1}} + I_{\mathrm{rm2}} + \cdots + I_{\mathrm{rmn}} \\ Q_{\mathrm{rrz}} = Q_{\mathrm{rr1}} + Q_{\mathrm{rr2}} + \cdots + Q_{\mathrm{rrn}} \\ \tau_z = \frac{Q_{\mathrm{rrz}}}{I_{\mathrm{rmz}}} - \frac{I_{\mathrm{rmz}}}{2K_z} \end{cases} \tag{3}$$

where K_z is the total decrease rate of parallel thyristors current, I_{rmz} is the total peak value of the reverse recovery current of parallel thyristors, Q_{rrz} is the total reverse recovery charge of parallel thyristors, and τ_z is the total reverse recovery current decay time constant.

IV. Commutating Equivalent Circuit Analysis

The circuit topology of converter unit (CU1–CU4) in Fig. 1 is shown in Fig. 4; E_A, E_B, and E_C is transformer secondary-side phase voltage, and L_s is the sum of the circuit stray inductance and transformer leakage inductance. There are 12 thyristors in parallel on each bridge arm.

Although each thyristor has its own RC snubber, as for the three-phase full-pulse bridge configuration, the different bridge-arm RC snubbers will interact with each other. When arm 1 thyristors turn-off, arms 2 and 3 are conducting and short-circuit their RC snubbers; however, thyristors 4, 5, and 6 are blocking and their RC snubbers will also interact with the arm 1 snubbers. The equivalent circuit is given in Fig. 5(a), and the voltage source in the circuit of Fig. 5(b) can be assumed to be a constant dc voltage E_{eq} because of the slow variation of power-frequency voltage E_{AB}, compared to the fast reverse recovery transients in this circuit

$$E_{\mathrm{eq}} = \sqrt{2} E_{\mathrm{AB}} \sin(\alpha + \mu) \tag{4}$$

$$C_{\mathrm{eq}} = 20 C_s \tag{5}$$

$$R_{\mathrm{eq}} = \frac{1}{20} R_s \tag{6}$$

$$L_{\mathrm{eq}} = 2 L_s \tag{7}$$

where α is the trigger delay angle and μ is the commutating overlapping angle. From the parameters listed in Table I, it is easy to get the results that $E_{AB} = 1000$ V and $L_{\mathrm{eq}} = 30\ \mu$H. The maximum commutating over-voltage occurs under the condition of $\alpha + \mu = 90°$, and thus E_{eq} equals 1414 V in the worst case.

The parallel thyristors can be modeled as a controlled current source, and then, the equivalent circuit given in Fig. 5(b) can be converted to the transient analysis circuit shown in Fig. 5(c).

It is very difficult to obtain the current decrease rate of each thyristor at design stage, but it is easy to get the the total decrease rate K_z as

$$K_z = \frac{E_{\mathrm{eq}}}{L_{\mathrm{eq}}} = 47.1\ \mathrm{A}/\mu\mathrm{s}. \tag{8}$$

Suppose dynamic current balance coefficient equals J according to the system specific condition; it is easy to get the maximum current decrease rate $K_{\max}$ as

$$K_{\max} = \frac{K_z}{12 \times J} = 4.9\ \mathrm{A}/\mu\mathrm{s}. \tag{9}$$

The higher current-decrease rate, the larger peak-reverse current and the higher commutating over-voltage; considering the worst case, each thyristor current decrease rate can be assumed as $K_{\max}$, the peak value of the reverse recovery current, and the reverse recovery charge of each thyristor can be obtained according to the reverse-recovery characteristic curve provided by the manufacturer, as shown in Figs. 6 and 7. It is easy to obtain that $I_{\mathrm{rm}} = 250$ A, $Q_{\mathrm{rr}} = 15\,000\ \mu$As. Thus, $I_{\mathrm{rmz}} = 250 \times 12 = 3000$ A, and $Q_{\mathrm{rrz}} = 15\,000 \times 12 = 180\,000\ \mu$As. The decay time constant of reverse recovery current equals to 28 μs, which be calculated by using (3). Therefore, the total reverse recovery current is modeled as

$$i_{\mathrm{rmz}} = -3000 e^{-\frac{t}{28 \times 10^{-6}}}. \tag{10}$$

The equation of circuit given in Fig. 5(c) can be expressed by using Kirchhoff's first law as follows:

$$L_{\mathrm{eq}} \frac{di}{dt} + R_{\mathrm{eq}}(i - i_{\mathrm{rmz}}) + \frac{1}{C_{\mathrm{eq}}} \int_0^t (i - i_{\mathrm{rmz}}) dt = E_{\mathrm{eq}}. \tag{11}$$

Letting

$$p = \frac{R_{\mathrm{eq}}}{2 L_{\mathrm{eq}}} \quad w = \frac{1}{\sqrt{L_{\mathrm{eq}} C_{\mathrm{eq}}}} \quad \xi = \frac{p}{w} = R_{\mathrm{eq}} / \left(2 \sqrt{\frac{L_{\mathrm{eq}}}{C_{\mathrm{eq}}}} \right)$$

equation (11) becomes

$$\frac{d^2 i}{dt^2} + 2p \frac{di}{dt} + w^2 i = w^2 \left(1 - \frac{2p}{\tau w^2} \right) i_{\mathrm{rmz}}. \tag{12}$$

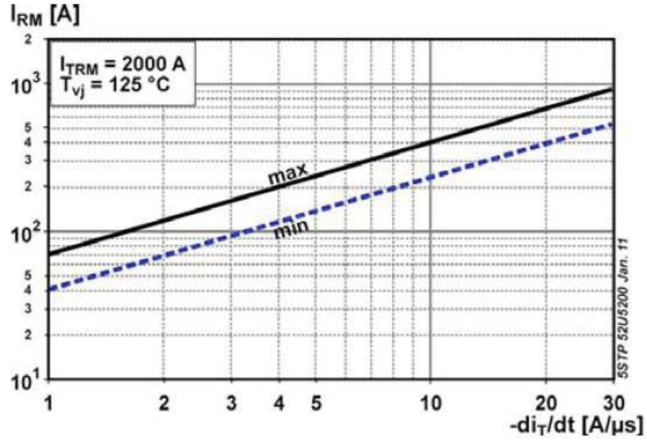

Fig. 6. Thyristor reverse recovery characteristics curve (I_{rm} versus di/dt).

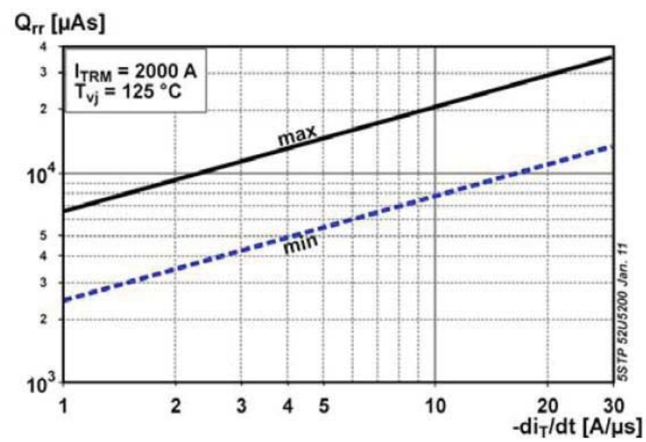

Fig. 7. Thyristor reverse recovery characteristics curve (Q_{rr} versus di/dt).

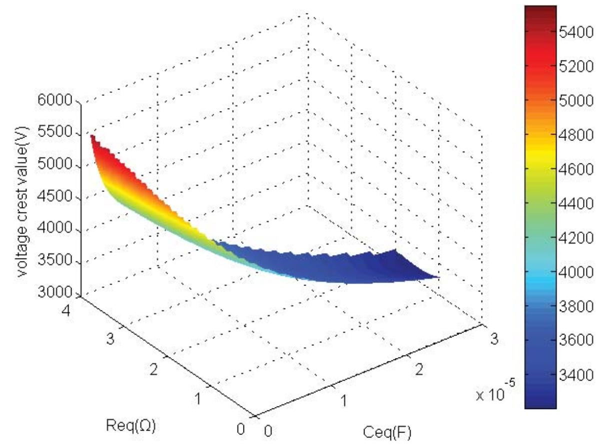

Fig. 8. Peak value of commutating over-voltage versus R_{eq}, C_{eq}.

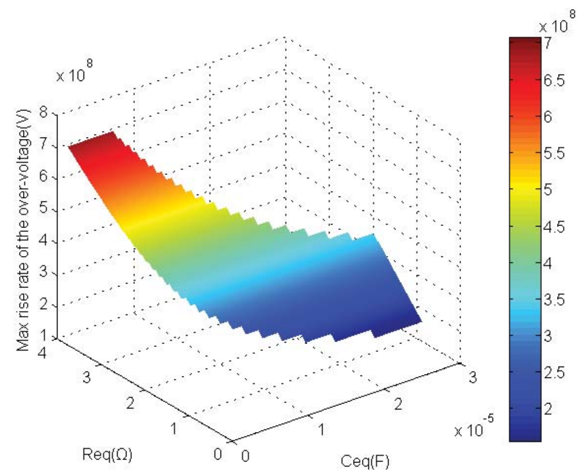

Fig. 9. Maximum rise rate of commutating over-voltage versus R_{eq}, C_{eq}.

V. SNUBBER PARAMETER DESIGN

Since (12) is a linear ordinary differential equation with constant coefficients, the optimal system-transient response needs enough speediness and damping, and therefore, the damp ratio ξ should be in the interval [0.4, 1]. Equation (12) can be solved in the under-damped case with proper initial conditions: inductance current equals I_{rmz} and capacitance voltage equals zero

$$i = (A_1 \cos bt + A_2 \sin bt)e^{-pt} + ge^{-\frac{t}{\tau}} \tag{13}$$

where

$$b = \sqrt{w^2 - p^2} \tag{14}$$

$$A_1 = I_{\mathrm{rmz}} - g \tag{15}$$

$$A_2 = -\frac{p(I_{\mathrm{rmz}} - g) + \frac{E_{\mathrm{eq}}}{L_{\mathrm{eq}}} + \frac{g}{\tau_z}}{b} \tag{16}$$

$$g = \frac{\tau_z\left(\tau_z - \frac{2p}{w^2}\right)I_{\mathrm{rmz}}}{\tau_z\left(\tau_z - \frac{2p}{w^2}\right) + \frac{1}{w^2}}. \tag{17}$$

The analytic expression of commutating over-voltage V_d and dV_d/dt can be obtained

$$V_d = E_{\mathrm{eq}} + L_{\mathrm{eq}}\left[\left(pA_1 - bA_2\right)\cos bt + \left(bA_1 + pA_2\right)\sin bt\right]e^{-12pt} + L_{\mathrm{eq}}\frac{g}{\tau_z}e^{-\frac{t}{\tau_z}} \tag{18}$$

$$\frac{dV_d}{dt} = L_{\mathrm{eq}}\left\{\left[\left(b^2 - p^2\right)A_1 + 2bpA_2\right]\cos bt + \left[\left(b^2 - p^2\right)A_2 - 2bpA_1\right]\sin bt\right\}e^{-pt} - L_{\mathrm{eq}}\frac{g}{\tau^2}e^{-\frac{t}{\tau}}. \tag{19}$$

The total turn-off loss of the circuit is

$$W_{\mathrm{tt}} = \int_0^{\infty} V_d i\, dt = E_{\mathrm{eq}}Q_{\mathrm{rrz}} + C_{\mathrm{eq}}E_{\mathrm{eq}}^2. \tag{20}$$

The proper combination of R_{eq}, C_{eq} values can be selected to meet the requirement of $0.4 < \xi < 1$ by using MATLAB program. According to (18) and (19), the peak value and the maximum dV_d/d_t of the thyristor commutating over-voltage under proper R_{eq}, C_{eq} combination are shown in Figs. 8 and 9.

According to the data sheet of the thyristor 5STP 52U5200, the maximum repetitive peak reverse voltage equals 5200 V, and the critical rate of rise of commutating voltage equals to 2×10^9 V/s. Considering the design safety margin, the peak

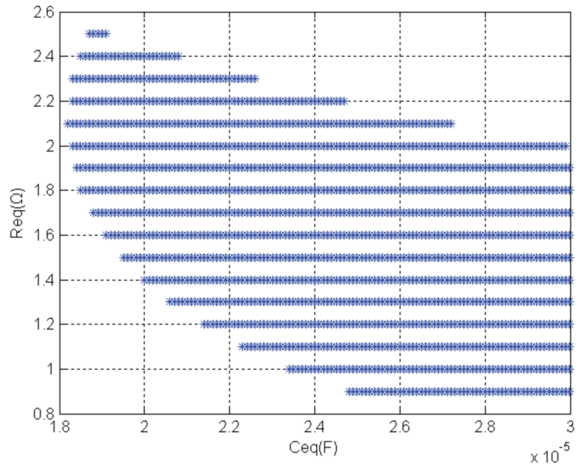

Fig. 10. Allowable R_{eq}, C_{eq} value combination.

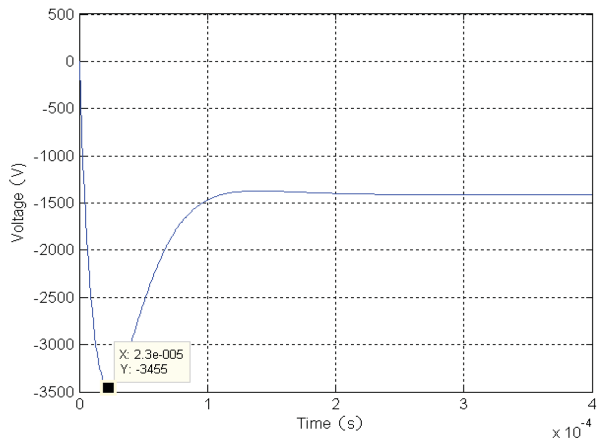

Fig. 11. Commutating over-voltage waveform calculated by MATLAB.

voltage value should be suppressed to less than 3500 V and the maximum dV_d/dt should be limited to less than 1×10^9 V/s. The proper combination of R_{eq}, C_{eq} values can be selected to meet the above requirement calculated by MATLAB program, as shown in Fig. 10.

As shown in the Fig. 8, the voltage peak value is mainly affected by capacitance; however, the voltage peak value does not change significantly when the capacitance value increases to a certain extent, and therefore, too large capacitance value is not meaningful to significantly reduce the peak voltage. On the other hand, commutating power loss increases linearly along with the capacitance addition according to (20), so the capacitance C_{eq} should be selected as 20 μF. When the thyristor turns on, the increase of resistor is beneficial to limiting the rise rate of the capacitor discharge current, and thus the resistor R_{eq} can be selected as 2.4 Ω; then, it is easy to know C_s equals 1 μF and R_s equals 48 Ω from (5) and (6). The waveform of the commutating over-voltage calculated by MATLAB is shown in Fig. 11—theoretical peak value equals 3455 V.

VI. CONCLUSION

There was a current transfer between the parallel thyristors due to the fact that each thyristor cannot turn off at the same time, so the exponential function model based on a single thyristor was not applicable any more. The parallel thyristors were assumed as one virtual thyristor, and then the reverse recovery current could be modeled by an exponential function model. Through the equivalent transformation of rectifier circuit, the commutating over-voltage, over-voltage rise rate, and snubber power loss were calculated based on the Kirchhoff's equation. Then, the RC value was selected as 48 Ω, 1 μF according to commutating over-voltage protection requirements, including the maximum allowable over-voltage value, the critical rate of rise of commutating voltage, and the reduction of snubber power loss.

VII. DISCLAIMER

The views and opinions expressed herein do not necessarily reflect those of the ITER organization.

ACKNOWLEDGMENT

The authors would like to thank Q. Zhou and Y. Wu, who were helpful in obtaining the thyristor data.

REFERENCES

[1] I. B. Mondino, L. Pier-Luigi, A. G. Roshal, A. Coletti, D. Hrabal, A. Maschio, R. Piovan, S. M. Tenconi, S. Bulgakov, and V. G. Kuchinski, "AC/DC converters for the ITER poloidal system," in *Proc. 16th IEEE/NPSS Symp. Fusion Eng. Seeking New Energy*, vol. 1. Oct. 1995, pp. 658–661.

[2] P. L. Mondino, T. Bonicelli, V. Kuchinskiy, and A. Roshal, "ITER research and development: Auxiliary systems: Coil power supply components," *Fusion Eng. Design*, vol. 55, pp. 325–330. Jan. 2001.

[3] P. Fu, G. Gao, L. W. Xu, Z. Q. Song, Z. C. Sheng, S. Jong-Seok, I. Benfatto, J. O. Tao, A. D. Mankani, and C. L. Neumeyer, "Review and analysis of the ac/dc converter of ITER coil power supply," in *Proc. 25th Annu. IEEE Appl. Power Electron. Conf. Exposit.*, Feb. 2010, pp. 1810–1816.

[4] J. Tao, I. Benfatto, J. K. Goff, A. D. Mankani, F. Milani, I. H. Song, H. Tan, and J. Thomsen, "ITER coil power supply and distribution system and distribution," in *Proc. IEEE/NPSS 24th Symp. Fusion Eng.*, Jun. 2011, pp. 1–8.

[5] G. Zou, X. X. Chen, J. C. Zheng, and C. Q. Wu. "A macro-model of SCR for transient analysis in power electronic system," in *Proc. Int. Conf. Power Syst. Technol.*, Aug. 1998. pp. 659–663.

[6] F. Gracia, F. Arizti, and F. Aranceta, "A nonideal macro-model of thyristor for transient analysis," *IEEE Trans. Ind. Electron.*, vol. 37, no. 6, pp. 514–520, Dec. 1990.

[7] C. L. Ma, P. O. Lauritzen, P. Turkes, and H. J. Mattausc, "A physically-based lumped-charge SCR model," in *Proc. IEEE 24th Power Electron. Spectr. Conf.*, Jun. 1993, pp. 53–59.

[8] R. S. Choknawala and E. I. Carroll, "A snubber design tool for P-N junction reverse recovery using a more accurate simulation of the reverse recovery waveform," *IEEE Trans. Ind. Appl.*, vol. 27, no. 1, pp. 74–84, Feb. 1991.

[9] S. B. Taib, L. N. Hulley, Z. Wu, and W. Shepherd, "Thyristor switch model for power electronic circuit simulation in modified SPICE 2," *IEEE Trans. Power Electron.*, vol. 7, no. 3, pp. 568–580, Jul. 1992.

[10] Y. Liang and V. Gosbell, "A versatile switch model for power electronics SPICE 2 simulations," *IEEE Trans. Ind. Electron.*, vol. 36, no. 1, pp. 86–88, Feb. 1989.

[11] T. M. Undeland, A. Petterteig, G. Hauknes, A. K. Adnanes, and S. Garberg, "Diode and thyristor turn-off snubbers simulation by KREAN and an easy to use design algorithm," in *Proc. IEEE. Ind. Appl. Soc. Annu. Meeting*, Oct. 1988. pp. 647–654.

[12] C. W. Lee and S. B. Park, "Determination of thyristor reverse recovery current parameters," *Electr. Power Appl.*, vol. 135, no. 2, pp. 1018–1021, Mar. 1987.

[13] C. W. Lee and S. B. Park, "Design of a thyristor snubber circuit by considering the reverse recovery process," *IEEE Trans. Power Electron.*, vol. 3, no. 4, pp. 440–446, Oct. 1988.
[14] J. Bernardes and S. Swindler, "Modeling and analysis of thyristor and diode reverse recovery in railgun pulsed power circuits," in *Proc. IEEE Pulsed Power Conf.*, Jun. 2005, pp. 79–82.

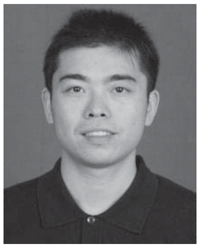

Fengwei Zha was born in Anhui, China, in 1977. He received the B.S. and M.S. degrees in electrical automation from the Anhui University of Technology, Maanshan, China, in 2000 and 2005, respectively. He is currently pursuing the Ph.D. degree in nuclear science and engineering with the Institute of Plasma Physics, Chinese Academy of Science, Hefei, China.

He is currently a Lecturer with the Anhui University of Technology. In 2009, he joined the Institute of Plasma Physics, Chinese Academy of Science. His current research interests include high-power pulse power sources and over-voltage protection.

Zhiquan Song was born in Anhui, China, in 1975. He received the B.S. degree in power supply system and automation from the Hefei University of Technology, Hefei, China, in 1999, and the Ph.D. degree in nuclear engineering from the Chinese Academy of Sciences, Hefei, in 2007.

He is currently an Engineer with the International Thermonuclear Experimental Reactor project with the Institute of Plasma Physics, Chinese Academy of Sciences, Hefei. His current research interests include power supply systems of fusion devices.

Fu Peng was born in Hubei, China, in 1962. He received the B.S. degree in electrical engineering from the Huazhong University of Science and Technology, Wuhan, China, in 1985, and the M.S. and Ph.D. degrees in electrical engineering from the Chinese Academy of Sciences, Hefei, China, in 1990 and 1997, respectively.

He is currently a Professor and a Manager of the International Thermonuclear Experimental Reactor project with the Institute of Plasma Physics, Chinese Academy of Sciences, Hefei. His current research interests include power supplies and their control systems of fusion devices.

Ling Dong was born in Hubei, China, in 1980. He received the B.S. degree in mechanism design from the Wuhan University of Technology Wuhan, China, in 2002, and the M.S. and Ph.D. degrees in mechanical engineering from University Louis Pasteur, Strasbourg, France, in 2004 and 2007, respectively.

He is currently a Deputy Director of the Division of Project Engineering, China International Nuclear Fusion Energy Program Execution Center. His current research interests include power supplies and their control systems of fusion devices.

Min Wang was born in Jiangxi, China, in 1980. She received the B.S. and M.S. degrees in electrical engineering from the Huazhong University of Science and Technology, Wuhan, China, in 1999 and 2004, respectively.